

Spotting Temporally Precise, Fine-Grained Events in Video

James Hong¹, Haotian Zhang¹, Michaël Gharbi²,
Matthew Fisher², and Kayvon Fatahalian¹

¹ Stanford University

² Adobe Research

Abstract. We introduce the task of spotting temporally precise, fine-grained events in video (detecting the precise moment in time events occur). Precise spotting requires models to reason globally about the full-time scale of actions and locally to identify subtle frame-to-frame appearance and motion differences that identify events during these actions. Surprisingly, we find that top performing solutions to prior video understanding tasks such as action detection and segmentation do not simultaneously meet both requirements. In response, we propose E2E-Spot, a compact, end-to-end model that performs well on the precise spotting task and can be trained quickly on a single GPU. We demonstrate that E2E-Spot significantly outperforms recent baselines adapted from the video action detection, segmentation, and spotting literature to the precise spotting task. Finally, we contribute new annotations and splits to several fine-grained sports action datasets to make these datasets suitable for future work on precise spotting.

Keywords: temporally precise spotting; video understanding

1 Introduction

Detecting the precise moment in time events occur in a video (temporally precise event ‘spotting’) is an important video analysis task that stands to be essential to many future advanced video analytics and video editing [67] applications. However, despite significant progress in fine-grained video understanding [12, 29, 44, 59], temporal action detection (TAD) [5, 11, 28, 47, 63], and temporal action segmentation (TAS) [20, 30, 53], precise event spotting has rarely been studied by the video understanding community.

We address this gap by focusing on the challenge of precisely spotting events in sports video. We study sports video because of the quantity of data available and the high temporal accuracy needed to analyze human performances. For example, we wish to determine the frame in which a tennis player hits the ball, the frame a ball bounces on the court, or the moment a figure skater starts or lands a jump. Figure 1 shows examples from these sports and illustrates why

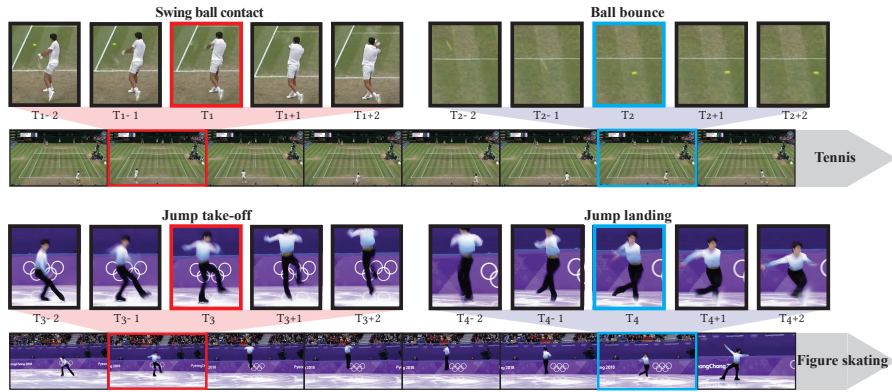


Fig. 1: We perform temporally precise spotting of events in video, where success requires detecting the occurrence of an event within a single or small tolerance of frames. Examples of precise events: in *tennis*, the moment a player contacts the ball during a swing (red) or when a ball bounces on the court (blue); in *figure skating*, the moment of take-off (red) and landing (blue) during a jump.

precise spotting is challenging. The goal is to identify the precise frame when an event occurs, but adjacent frames are extremely similar visually; looking at one or two frames alone, it can be difficult even for a human to judge when a racket makes contact with a ball or when a figure skater lands a jump. However, inspection of longer sequences of frames makes the task significantly more tractable since the observer knows when to expect the event of interest in the context of a longer action (e.g., the swing of the racket, the preparation for a jump, or a ball’s trajectory). Therefore, we hypothesize that precise spotting requires models that can (1) represent subtle appearance and motion clues, and also (2) make decisions using information spread over long temporal contexts.

Surprisingly, we have found that the large body of literature on video understanding lacks solutions that meet these two requirements in the regime of temporally precise spotting. For example, action recognition (classification) models are not designed to operate efficiently on large temporal windows and struggle to learn in the heavily class-imbalanced setting created by precise spotting of rare events. Sequence models from segmentation and detection extract patterns over longer timescales, but training these complex models end-to-end has led to optimization challenges. This has resulted in many solutions that operate in two phases, relying on pre-trained (or modestly fine-tuned) input features that are not particularly specialized to capture the subtle (and often highly domain-specific) visual details needed to spot events with temporal precision.

We propose a simpler alternative (E2E-Spot) to satisfy our hypothesized requirements. The key to training a sequence model end-to-end over a wide temporal context is an efficient per-frame feature extractor that can process hundreds of contiguous frames without exceeding platform memory. We demonstrate how

to combine existing modules from the video processing literature to accomplish this goal without introducing new, bespoke architectures.

Despite its simplicity, E2E-Spot significantly outperforms prior baselines, which opt for a two-phase approach, as well as naive end-to-end learning approaches on precise spotting. Moreover, E2E-Spot is computationally efficient at inference time and can complete the full end-to-end spotting task in less time than just the feature extraction phase of many prior methods [2, 6].

This paper makes three main contributions:

1. The novel task of temporally precise spotting of fine-grained events. We introduce frame-accurate labels for two existing fine-grained sports action datasets: Tennis [67] and Figure Skating [25]. We also adapt the temporal annotations from FineGym [44] and FineDiving [61] to show the generality of the precise spotting task.
2. E2E-Spot, a from-the-ground-up, end-to-end learning approach to precise spotting that combines well-established architectural components [8, 43, 54] and can be trained quickly on a single GPU.
3. Analysis of spotting performance. E2E-Spot outperforms strong baselines (§ 5) on precise temporal spotting (by 4–11 mAP, spotting within 1 frame). E2E-Spot is also competitive on coarser spotting tasks (within 1–5 sec), achieving second place in the 2022 SoccerNet Action Spotting challenge [13, 14] (within 1.1 avg-mAP) and a lift of 14.8–16.5 avg-mAP over prior work.

Our code and data are publicly available.

2 Related Work

Action Spotting. Previous work on spotting [13] focuses on *coarse* action spotting, where a detection is deemed correct if it occurs within some time-window around the true event, with a loose error tolerance (1–5 or 5–60 seconds, equating to 10–100s of frames). On the Tennis [67] and Figure Skating [25] datasets described in § 4, a spotting error larger than 1–2 frames is essentially equivalent to missing the event altogether (e.g., a ball impact’s on the ground; Figure 1). For demanding applications that require precise temporal annotations, we argue the relevant task is *precise* event spotting, where detection thresholds are much more stringent tolerances (1–5 frames; as little as 33 ms in 25–30 FPS video). We use a similar metric to coarse action spotting: mean Average Precision (mAP @ δ) but with a short temporal tolerance δ .

Temporal Action Detection (TAD) and Segmentation (TAS) localize *intervals*, often spanning several seconds and containing an ‘action’. Depending on the dataset, these can be atomic actions such as “standing up” [47] or broad activities such as “billiards” [28]. For such action definitions, it is often unclear what would be considered a temporally precise event to spot.

The success criteria for TAD and TAS also differ from that of precise spotting. TAD [5, 11, 28, 47, 63] is evaluated on interval-based metrics such as mAP @

temporal Intersection-over-Union (IoU) or at sub-sampled time points, neither of which enforce frame accuracy on the action boundaries. Down-sampling in time (up to $16\times$) is a common preprocessing step [3, 36, 37, 45, 62, 66]. TAS [20, 30, 53] also optimizes interval-based metrics such as F1 @ temporal overlap. Frame-level metrics for TAS reward accuracy on densely labeled, intra-segment frames; in contrast, event frames in our spotting datasets are sparse. Spatial-temporal detection benchmarks [31, 33] differ from standard TAD, TAS, and precise spotting by combining both spatial and temporal IoU [33].

Recent approaches for TAD [10, 36, 37, 56, 62, 65] and TAS [1, 7, 19, 27, 50, 64] often proceed in two stages: (1) feature extraction then (2) head learning for the end task. Fixed, pre-trained features from video classification on Kinetics-400 are often used for the first stage [2, 6, 60], and state-of-the-art TAD methods with these features [39, 66, 69] often perform comparably to if not better than recent end-to-end learning approaches [34, 38]. Indirect fine-tuning using classification in the target domain is sometimes performed to improve feature encoding [2, 45]. Early end-to-end approaches encode video as non-overlapping segments [3] (e.g., 16 frames) or downsample in time [46, 48], producing features that are too temporally coarse to be effective for spotting frame-accurate events.

Like TAD and TAS, precise spotting is a temporal localization task performed on untrimmed video. As is the case, many models for TAD and TAS can be adapted for precise spotting. We use MS-TCN [19], GCN [62], GRU [8], and AS-Former [64] as baselines, and we test these models with different features [2, 6, 18] in § 5. However, we find that relying on fixed or indirectly fine-tuned features as input for these models is a critical limitation. Our experiments show that (1) E2E-Spot is a strong baseline for precise spotting and (2) more complex architectures do not necessarily provide additional benefit when feature learning is end-to-end. Finally, we note the long history of CNN-RNN architectures in TAD/TAS [3, 4, 16, 49, 63]; E2E-Spot is a simple design from this family, motivated by our requirements for frame-dense processing and end-to-end learning, and implemented using a modern CNN for spatial-temporal feature encoding.

Video Classification predicts one label for an entire video, as opposed to per-frame labels for spotting. This leads to two key differences: (1) sparsely sampling frames [21, 60] is effective, whereas precise spotting requires dense sampling; (2) to obtain a video-level prediction, popular architectures for classification typically perform global space-time pooling [58] or temporal consensus [35, 60, 70]. E2E-Spot shows that omitting temporal pooling³ and training end-to-end yields an efficient pipeline for precise, per-frame spotting.

E2E-Spot incorporates ideas from popular video classification models for spatial-temporal feature extraction. TSM [35] introduced the temporal shift operation, which converts a 2D CNN into a spatial-temporal feature extractor by mixing channels between time steps. GSM [54] learns the shift. We find the combination of RegNet-Y [43] and GSM [54] to be effective and suggest these building blocks as a starting point for future spotting research.

³ Omission of temporal pooling is similar to concurrent work, E2E-TAD [38].

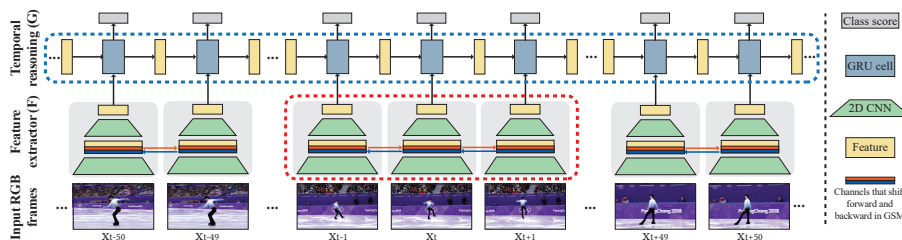


Fig. 2: **Overview of E2E-Spot.** RGB video frames are first input to a local spatial-temporal feature extractor F (a RegNet-Y [43] with GSM [54]) to produce a feature for each frame that captures subtle differences and motion across neighboring frames (red dotted box). The feature sequence is then processed by a sequence model G , which builds a long-scale temporal context (blue dotted box; one direction drawn) and outputs a class prediction for every frame.

Sports Activity Datasets are a fertile testing ground for video action recognition and understanding [13, 24–26, 32, 33, 44, 61, 67]. We evaluate using temporal annotations from several recent datasets [13, 25, 44, 61, 67]. These datasets are fine-grained, meaning that all event and class labels relate to a single activity (i.e., a single sport), as compared to coarse-grained datasets [5, 28], where classes comprise a broad mix of generic activities. Supporting fine-grained concepts and labels is an important requirement of many practical, real-world applications.

3 E2E-Spot: An End-to-End Model for Precise Spotting

We define the precise temporal event spotting task as follows: given a video with N frames $\mathbf{x}_1, \dots, \mathbf{x}_N$ and a set of K event classes $\mathbf{c}_1, \dots, \mathbf{c}_K$, the goal is to predict the (sparse) set of frame indices when an event occurs, as well as the event’s class $(t, \hat{\mathbf{y}}_t) \in \mathbb{N} \times \{\mathbf{c}_1, \dots, \mathbf{c}_K\}$. A prediction is deemed correct if its timestamp falls within δ frames of a labeled ground-truth event and it has the correct class label. In precise spotting, the temporal tolerance δ is small — i.e., a few frames only. We assume that the frame rate of the video is sufficiently high to capture the precise event and that frame rates are similar across videos.

We identified several key design requirements for a model to perform well on the temporally precise spotting task:

1. Task-specific **local spatial-temporal features** that capture subtle visual differences and motion across neighboring frames.
2. A **long-term temporal reasoning** mechanism, which provides a long temporal window to spot short, rare events. For instance, it is difficult to identify the precise time a figure skater enters a jump from a handful of frames. But spotting becomes much less ambiguous given the wider context of the acceleration (before) and landing (after the jump) (see Figure 1). These contexts can occur over many seconds and frames.

3. Dense frame prediction at the temporal granularity of a single frame.

These requirements call for an expressive and efficient network architecture that can be trained end-to-end via direct supervision on spotting.

E2E-Spot treats a video classification network (with global temporal pooling removed) as part of a sequence model, so that processing a clip of N frames results in N output features and N per-frame predictions. Figure 2 illustrates our pipeline. Frames from each RGB video are first fed to a local spatial-temporal feature extractor F , which produces a dense feature vector for each frame (§ 3.1). This lightweight feature extractor incorporates Gate Shift Modules (GSM) [54] into a generic 2D convolutional neural network (CNN) [43]. The feature sequence is then further processed by a sequence model G , which builds a long-scale temporal context and outputs a class prediction for every frame, including a ‘background’ class to indicate when no event was detected (§ 3.2).

3.1 Local Spatial-Temporal Feature Extractor, F

The first stage of our pipeline extracts spatial-temporal features for each frame. We strive to keep the feature extractor as lightweight as possible, but found that a simple 2D CNN that processes frames independently [9, 22, 57, 60] is often insufficient for precise spotting (see § 5.2). This is because a 2D CNN does not capture the spatially-local temporal correlations between frames. In videos that are densely sampled (24–30 FPS), this temporal signal is critical to learn features that can robustly differentiate otherwise very similar frames: for instance, the speed and travel direction of a tennis ball, when each frame likely exhibits motion blur. To obtain more expressive, motion-sensitive features we implement F as a 2D CNN with Gate Shift Modules (GSM) [54]. We choose RegNet-Y [43], a recent and compact CNN, as the 2D backbone.

Our feature extractor is similar to models for video classification [35, 54, 60], but with two key differences: (1) it samples frames *densely* and (2) it uses no final temporal consensus/pooling because our goal is to obtain one output per frame, rather than one for the whole video or multi-frame segment.

Efficiency Compared to Other Per-frame Feature Extractors. A common alternative for per-frame feature extraction [2, 19] is to stride a video classification model densely — i.e., by using a model which takes M frames as input and produces a single feature and by running it on the M frame neighborhood of every frame. The overhead of processing each frame multiple times in overlapping windows makes end-to-end feature learning or fine-tuning difficult for tasks like spotting that require dense processing of frames. In contrast, our approach processes each frame once and can be trained as part of an end-to-end pipeline with much longer sequences (100s of frames), even on a single GPU (see Table 1).

3.2 Long-term Temporal Reasoning Module, G

To gather long-term temporal information, we use a 1-layer bidirectional Gated Recurrent Unit (GRU [8]) network G , which processes the dense per-frame fea-

Table 1: **E2E-Spot efficiency and throughput.** We compare the model complexity, the maximum batch size for *end-to-end training on 100 frame clips* (at 224×224), and per-frame inference time on a Nvidia A5000 GPU with 24GB of VRAM [42]. E2E-Spot is significantly faster at inferring features than striding a video classification model and allows for practical end-to-end trained spotting.

Architecture	Params (M)	Max batch size	Inference time (ms)
E2E-Spot: RegNet-Y 200MF w/ GSM + GRU	(2.8 + 1.7)	18	0.3
E2E-Spot: RegNet-Y 800MF w/ GSM + GRU	(5.5 + 7.1)	8	0.6
<i>Comparison to other feature extractors: (* := exceeds GPU memory)</i>			
RegNet-Y 200MF w/ GSM (7 frames per window)	2.8	2	1.6
RegNet-Y 200MF w/ GSM (15 frames per window)	2.8	1	3.2
I3D (21 frames; used by [19])	12.3	*	8.5
R(2+1)D-34 [58] (12 frames, 128×128 ; used by [2])	63.7	*	11.0
ResNet-152 (1 frame only; used by [9, 22, 57])	60.2	2	1.8
Feature combination (for SoccerNet-v2) [71]	>200	-	-

tures produced by F . We set the hidden dimension of G to match that of F . Finally, we apply a fully connected layer and softmax on the GRU outputs to make a per-frame $K+1$ way prediction (including 1 ‘no-event’ background class).

We found that a single-layer GRU suffices and that more complex sequence models such as MS-TCN [19] or a deeper GRU do not necessarily improve accuracy (see § 5.2). We hypothesize that as a result of end-to-end training, the features produced by F capture subtle temporal cues that are specific to a given activity’s and task’s requirements. This shifts the burden of representations to F so that G only needs to propagate the temporal context.

3.3 Per-frame Cross-Entropy Loss

For a N -frame clip, we output a sequence of N class scores — i.e. a $(K+1)$ -dimensional vector $\hat{\mathbf{y}}_t$ for each frame t , accounting for the background class:

$$(\hat{\mathbf{y}}_1, \dots, \hat{\mathbf{y}}_N) = G \circ F(\mathbf{x}_1, \dots, \mathbf{x}_N). \quad (1)$$

Each frame has a ground-truth label $\mathbf{y}_t \in \{\mathbf{c}_1, \dots, \mathbf{c}_K\} \cup \{\mathbf{c}_{background}\}$ encoded as a one-hot vector. We optimize per-frame classification with cross-entropy loss:

$$l(\mathbf{x}_1, \dots, \mathbf{x}_N) = \sum_{t=1}^N \text{CE}(\hat{\mathbf{y}}_t, \mathbf{y}_t) \quad (2)$$

3.4 Implementation Details

We conduct experiments with two versions of F utilizing RegNet-Y 200MF and 800MF (MF refers to MFLOPs [43]). These CNN backbones are initialized with pre-trained weights from ImageNet-1K [15]. Details of the complexity and throughput of these models is given in Table 1.

We train E2E-Spot on 100-frame-long clips sampled randomly and use standard data-augmentations (e.g., crop, jitter, and mixup [68]). Frames are resized to 224 pixels in height and cropped to 224×224 unless otherwise stated (see supplement § A). We optimize using AdamW [41] and LR annealing [40]. To mitigate imbalance arising from the rarity of precise events ($< 3\%$ of frames), we boost the loss weight of the foreground classes ($5\times$) relative to the background.

At test time, we disable data-augmentation and overlap clips by 50%, averaging the per-frame predictions. To convert per-frame class scores into a set of spotting predictions, we rank all of the frames by their predicted score for each class. We follow standard procedure from coarse spotting [13] and other detection tasks [23] by reporting our results with non-maximum suppression (NMS). Empirically, we found NMS’s efficacy to vary by model and dataset (see Table 2). Refer to supplement § A for more implementation details.

4 Datasets

We evaluate precise spotting on four fine-grained sports video datasets with frame-level labels: Tennis [67], Figure Skating [25], FineDiving [61], and FineGym [44]. For full details about these datasets, please refer to supplement § D.

Tennis is an extension of the dataset from Vid2Player [67]. It consists of 3,345 video clips from 28 tennis matches (each clip is a ‘point’), with video frame rates of either 25 or 30 FPS. The dataset has 33,791 frame-accurate events divided into six classes: “player serve ball contact,” “regular swing ball contact,” and “ball bounce” (each divided by near- and far-court). Video from 19 matches are used for training and validation, while 9 matches are held out for testing.

Figure Skating [25] consists of 11 videos (all 25 FPS) containing 371 short program performances from the Winter Olympics (2010–2018) and World Championships (2017–2019). We refine the original labels by manually (re-)annotating the take-off and landing frames of jumps and flying spins, resulting in 3,674 event annotations across four classes. We consider two splits for evaluation:

- *Competition split* (FS-Comp): holds out all videos from the 2018 season for testing [25]. This split tests generalization to new videos (e.g., the next Olympics), despite domain-shift such as a new background in a new venue.
- *Performance split* (FS-Perf): stratifies each competition across train / val / test. This split tests a model’s ability to learn precise temporal events (by different skaters) without the background bias of the previous split.

FineDiving [61] contains 3,000 diving clips with temporal segment annotations. We spot the step transition frames for four classes, which include transitions into somersaults (pike and tuck), twists, and entry.

FineGym [44] contains 5,374 gymnastics performances, each treated as an untrimmed video. It has 32 spotting classes, derived from a hierarchy of action categories (e.g., balance beam dismounts; floor exercise turns). The original annotations denote the start and end of actions; we treat these boundaries as events — for instance, “balance beam dismount start” and “balance beam dismount

end”. We ignore the original splits, which are designed for action recognition and have overlap in videos, and we propose a 3:1:1 split between train / val / test. To reduce the variation in the frame rates of the source videos (which are 25–60 FPS), we resample all 50 and 60 FPS videos to 25 and 30 FPS, respectively.

Upon inspecting the FineGym labels for frame accuracy, we found the annotations for action start frames to be more visually consistent than those for end frames. For example, unlike in the Figure Skating dataset, the end frame is often several frames after the frame of landing for a jump. Thus, we also report results for a subset, FineGym-Start, which contains only start-of-action events.

5 Evaluation

In § 5.1, we demonstrate that the quality of per-frame feature representations extracted from the video has the greatest impact on results, rather than the choice of head architecture, and that end-to-end learning with E2E-Spot outperforms methods using pre-trained or indirectly fine-tuned features. In § 5.2 and § 5.3 we analyze the effect of temporal context, the importance of temporal modeling, and additional variations of E2E-Spot. In § 5.4 we report results on SoccerNet-v2, a temporally coarser spotting task.

Evaluation Metric. We measure Average Precision within a tolerance of δ frames (AP @ δ). AP is computed for each event class, and mAP is the mean across classes. We focus on tight tolerances such as $\delta = 1$ and $\delta = 2$. Precise temporal events are rare as a percentage of frames (0.2–2.9%), so metrics such as frame-level accuracy are not meaningful for precise spotting.

Baselines. We evaluate E2E-Spot against recent baselines from TAS, TAD, and coarse spotting that we adapted to the precise spotting task. These methods are not trained end-to-end; they adopt a two-phase separation between feature extraction and head training (i.e., downstream model) for the end-task. We form our baselines by pairing a *feature extraction strategy* with a *spotting head*. The latter is trained on extracted features to perform precise spotting, using the per-frame loss from Equation 2. See supplement § B for implementation details.

The baselines use the following head architectures: MS-TCN [19], GRU [8], ASFormer [64] from TAS; GCN [62] from TAD; and NetVLAD++ [22] and transformer [71] from action spotting. MS-TCN, GRU, and ASFormer performed best in our experiments, so we relegate results from the remaining architectures to supplement § C.1. We further attempt to boost the performance of these baselines using additional losses from the spotting literature, such as CALF [9] and label dilation⁴, and by post-processing using non-maximum suppression (within ± 1 frames). We report results from the best configuration of each baseline.

We pair each head architecture with pre-extracted input features, grouped into three broad categories:

⁴ Label dilation is defined as naive propagation to $[-1, +1]$ frames to mitigate sparsity.

1. *Pre-trained features* from video classification on Kinetics-400 [29], which are often used without any fine-tuning for TAD and TAS. Like Farha et al. [19], we extract per-frame I3D features by densely striding a 21-frame window around each frame. To test the impact of better pre-trained models, we also extract features with MViT-B [18], a state-of-the-art model from 2021.
2. *Fine-tuned features* using TSP [2] and $(K + 1)$ -way clip classification⁵. These features come from a classifier trained to predict whether a small window (e.g., 12 frames) contains an event, and they have the benefit of being adapted to the target video domain (e.g., tennis, skating, gymnastics).
3. *Pose features* (VPD) for the Figure Skating dataset only, which utilize a hand-engineered pipeline for subject tracking and fine-tuning [25]. *These features utilize domain-knowledge and are costly to develop for new datasets*, which may include phenomena not captured by pose (e.g., ball bounce in tennis). In activities such as figure skating, defined heavily by human motion, VPD features serve as a ceiling for E2E-Spot, which is domain agnostic.

Finally, we add a naive, end-to-end learned baseline that adapts video classification directly to the spotting task (VC-Spot). VC-Spot is given a 15-frame clip and tasked to predict whether the middle frame is a precise event. This baseline is to show that precise spotting is a distinct task from video classification.

5.1 Spotting Performance

We present two variations of E2E-Spot in the main results: (1) a default configuration with a RegNet-Y [43] 200MF CNN backbone and RGB input only, and (2) a configuration using RegNet-Y 800MF with RGB and flow input.

E2E-Spot with a 200MF CNN and RGB inputs consistently outperforms all non-pose baselines, while being comparable to the pose ones. The benefits of E2E-Spot are most striking at the most stringent tolerance, $\delta = 1$ frame (Table 2e). We summarize the key takeaways of our evaluation below.

Pre-trained features generalize poorly when no fine-tuning is used, regardless of the head architecture: between 9.1–29.1 worse than E2E-Spot in mAP at $\delta = 1$ (Table 2a). *Fine-tuning yields a significant improvement* over pre-trained features: between 3.9–25.1 mAP at $\delta = 1$ (Table 2b), indicating a large domain gap between Kinetics and the fine-grained spotting datasets. However, *E2E-Spot further outperforms the two-phase approaches with fine-tuned features* by 3.3–6.8 mAP, showing that indirect fine-tuning strategies for temporal localization tasks should be compared against directly supervised, end-to-end learned baselines. Finally, the wide variation in baseline performance (by sport) highlights the importance of evaluating new tasks, such as precise spotting, and their methods on a visually and semantically diverse set of activities and datasets.

VC-Spot performs poorly compared to E2E-Spot (Table 2d), especially on Figure Skating and FineGym, which require temporal understanding at longer timescales (e.g., several seconds) compared to Tennis and FineDiving.

⁵ For direct comparison, $(K + 1)$ -VC uses the same RegNet-Y 200MF w/ GSM CNN backbone as E2E-Spot. See supplement § B for details.

Table 2: **Spotting performance (mAP @ δ frames)**. The top results in each category and each column are underlined. SOTA is **bold**. We report best results under the following: † indicates NMS; * indicates CALF [9] or dilation. (e) E2E-Spot, trained with RGB only, generally outperforms the non-pose baselines and is competitive with the pose baselines on Figure Skating. E2E-Spot can further be improved with a larger 800MF CNN and a 2-stream ensemble with flow.

Feature	Model	Tennis		FS-Comp		FS-Perf		FineDiving		FG-Full		FG-Start	
		$\delta=1$	2	1	2	1	2	1	2	1	2	1	2
<i>(a) Pre-trained features (from Kinetics-400)</i>													
I3D [6]	MS-TCN	62.7 †*75.4	60.8 †*79.5	*69.0 †*89.3	-	-	-	-	-	-	-	-	-
(RGB & flow)	GRU	†*45.7 †*70.5	*41.8 †*69.8	*52.5 †*77.5	-	-	-	-	-	-	-	-	-
	ASFormer	*58.1 †*76.5	<u>61.2 †*82.4</u>	<u>69.0 †*89.7</u>	-	-	-	-	-	-	-	-	-
MViT-B [18]	MS-TCN	<u>67.0 †*80.1</u>	*57.4 †*79.9	*64.8 †*84.3	*59.3 †*78.3	†31.0 †*48.6	†41.7 †*64.8						
(RGB)	GRU	64.8 †* <u>80.8</u>	45.6 †*73.1	56.8 †*79.1	57.3	76.7 †*28.5 †* <u>48.6</u>	†*39.1 †*62.2						
	ASFormer	*63.9 †79.9	55.8 †*81.8	*56.5 †*81.7	*38.5 †*67.4	†*25.3 †*42.9	†*32.5 †*55.3						
<i>(b) Fine-tuned features</i>													
TSP [2]	MS-TCN	*90.9 †*95.1	72.4 †*87.8	*76.8	*89.9	*57.7	†76.0	†40.5	†58.5	†53.9	†*73.5		
(RGB)	GRU	89.5 †*96.0	*68.4 †*88.3	75.5	†*90.6	*57.0	*78.2	†38.7	†*58.8	†*53.2	†*74.2		
	ASFormer	89.8 †*95.5	<u>77.7 †94.1</u>	<u>80.2 †94.5</u>	*51.3	†*77.4	†38.8	†57.6	†51.1	†*72.9			
(K + 1)-VC	MS-TCN	91.1 †*95.1	66.5 †77.2	*77.2	†*89.9	<u>63.2 †*83.5</u>	†40.9	†*58.2	†53.2	†*73.8			
(RGB)	GRU	†*91.5 †* <u>96.2</u>	†61.7 †*78.9	†*76.8	†*89.4	*61.8 †*82.6	†41.1	†57.9	†54.3	†*73.6			
	ASFormer	<u>92.1 †*96.2</u>	*67.6 †*79.8	77.1	†*89.8	*58.9 †*83.5	†40.0	†*56.9	†53.6	†*72.9			
<i>(c) Hand-engineered tracking & pose features (top scores shown; see supplement § C for GRU and ASFormer)</i>													
2D-VPD [25]	MS-TCN	-	-	*83.5 †*96.2	*85.2 †*96.4	-	-	-	-	-	-	-	-
<i>(d) VC-Spot: video classification baseline using RGB</i>													
RegNet-Y 200MF w/ GSM		†92.4	†96.0	†61.8	†75.5	†56.2	†75.3	†62.4	†85.6	†18.7	†28.6	†25.9	†38.3
<i>(e) E2E-Spot</i>													
Default: 200MF (RGB)		96.1	†97.7	†*81.0	†*93.5	†*85.1	†*95.7	68.4	†85.3	†47.9	†65.2	†61.0	†78.4
Best: 800MF (2-stream)		† 96.9	† 98.1	†*83.4	†*94.9	†*83.3	†*96.0	†66.4	†84.8	†51.8	†68.5	†65.3	†81.6

E2E-Spot achieves similar results to pose features (2D-VPD [25]) on Figure Skating, within 0.1–2.5 mAP at $\delta = 1$. This is encouraging because E2E-Spot assumes no domain knowledge and is a more generally applicable approach.

Table 2e also shows E2E-Spot’s *best configuration*, using the larger 800MF CNN and both RGB and flow [55]. Neither of these enhancements (e.g., a larger CNN or flow) require domain knowledge, but can provide a small boost to the final performance over our 200MF defaults (0.8 mAP on Tennis and 3.9–4.3 mAP on FineGym). Details for other E2E-Spot configurations are presented in § 5.3.

5.2 Ablations of E2E-Spot

We analyze the requirements of precise spotting with respect to temporal context and network architecture. Refer to supplement § C for additional ablations.

Sensitivity to Clip Length. As a sequence model, E2E-Spot can benefit from and make stateful predictions over a long temporal context (e.g., 100s of frames). A long clip length allows for greater temporal context for each prediction, but linearly increases memory utilization per batch. We consider the number of frames needed for peak accuracy and train E2E-Spot with different clip lengths. Table 3a shows that different activities require different amounts of temporal context; the fast-paced events in Tennis can be successfully detected even when context is

Table 3: **Ablation and analysis experiments (mAP @ $\delta = 1$).** We compare to E2E-Spot defaults in the top row (RegNet-Y 200MF w/ GSM and GRU). (a) Varying clip lengths show that temporal context from longer clips is generally helpful. (b) Removing temporal information in the feature extractor F (GSM) and in the stateful predictions G (GRU) generally reduces mAP. (c) Reducing input resolution from 224 to 112 pixels reduces mAP. (d) More complex models for G than the 1-layer GRU do not significantly improve mAP. (e) Enlarging F to 800MF and/or adding flow can improve mAP slightly on some datasets.

Experiment		Tennis mAP Δ	FS-Comp mAP Δ	FS-Perf mAP Δ	FineDiving mAP Δ	FineGym-Full mAP Δ
E2E-Spot default: clip length = 100		96.1	†81.0	†85.1	68.4	†47.4
(a)	clip length = 8	†95.8 -0.3	†73.7 -7.3	†74.7 -10.4	†67.3 -1.1	†32.3 -15.1
	clip length = 16	†96.2 +0.1	†74.4 -6.6	†80.1 -5.0	†64.8 -3.6	†40.8 -6.6
	clip length = 25	†96.2 +0.1	†74.5 -6.5	†80.6 -4.5	†67.2 -1.2	†43.9 -3.5
	clip length = 50	†96.4 +0.3	†76.9 -4.1	†82.3 -2.8	65.0 -3.4	†46.6 -0.8
	clip length = 250	96.4 +0.3	†81.3 +0.3	†85.6 +0.5	68.9 +0.5	†48.5 +1.1
	clip length = 500	95.9 -0.2	†78.9 -2.1	†87.5 +2.4	-	†48.1 +0.7
(b)	w/o GRU	†95.7 -0.4	†74.3 -6.7	†77.9 -7.2	64.1 -4.3	†32.9 -14.5
	w/ TSM [35] instead of GSM	96.1 +0.0	†78.6 -2.4	†83.3 -1.8	†65.3 -3.1	†48.1 +0.7
	w/o GSM	†94.1 -2.0	†75.5 -5.5	†85.6 +0.4	68.9 +0.5	†44.2 -3.2
	w/o GSM & GRU	†60.1 -36.0	†26.9 -54.1	†41.1 -44.0	†47.0 -21.4	†22.1 -25.3
(c)	w/ 112 px resolution (height)	†88.5 -7.6	†75.4 -5.6	†80.9 -4.2	†64.9 -3.5	†45.3 -2.6
(d)	w/ MS-TCN	95.7 -0.4	†77.6 -3.4	†84.7 -0.4	67.0 -1.4	†44.1 -3.3
	w/ ASFormer	95.7 -0.4	†68.4 -12.6	†75.4 -9.7	70.4 +2.0	†36.8 -10.6
	w/ Deeper GRU	96.5 +0.4	†80.2 -0.8	†83.5 -1.6	67.2 -1.2	†46.4 -1.0
	w/ GRU* (see supplement)	96.2 +0.1	†78.1 -2.9	†86.0 +0.9	67.4 -1.0	†47.9 +0.5
(e)	200MF (Flow)	†58.2 -37.9	†72.4 -8.6	†76.6 -8.5	†60.7 -7.7	†44.4 -3.0
	200MF (RGB + flow; 2-stream)	†96.3 +0.2	†82.2 +1.2	†85.1 +0.0	†70.1 +1.7	†49.0 +1.6
	800MF (RGB)	96.8 +0.7	†84.0 +3.0	†83.6 -1.5	64.6 -3.8	†50.1 +2.7
	800MF (Flow)	†59.2 -36.9	†74.9 -6.1	†74.2 -10.9	†59.8 -8.6	†46.9 -0.5
	800MF (RGB + flow; 2-stream)	†96.9 +0.8	†83.4 +2.4	†83.3 -1.8	†66.4 -2.0	†51.8 +4.4

only 8–16 frames. In contrast, Figure Skating and FineGym show a clear drop in performance when clip length is reduced from 100 frames. Even longer clip lengths may be desirable (e.g., 250 frames), though with diminishing returns.

Value of Temporal Information in the Per-frame Features. E2E-Spot incorporates temporal information both in the 2D CNN backbone F (with GSM) and after global spatial-pooling in G (with GRU). We show the criticality of both of these components in Table 3b at $\delta = 1$. With neither GSM nor the GRU, the spotting task becomes a single-image classification problem; as expected, the results are poor (at least -21 mAP). The best results are achieved with both GSM and the GRU, except on FS-Perf and FineDiving, where results with and without GSM are similar. Replacing GSM with TSM [35] (fixed shift) ranges from comparable to worse, showing GSM to be a reasonable starting default.

Spatial Resolution. Lowering spatial resolution [34, 38] can speed up end-to-end learning and inference but degrades mAP on precise spotting (Table 3c), where the subjects may, at times, occupy only a small portion of the frame.

Table 4: **Average-mAP @ t for tolerances in seconds.** SOTA in **bold**. We show the top results from the CVPR 2021 and 2022 SoccerNet Action Spotting challenges. ‡ indicates challenge results — trained on the train, validation, and test splits. Shown and unshown refer to whether actions are visible; E2E-Spot is better at detecting the former, but Soares et al. [51] is superior at the latter.

Average-mAP @ tolerances	Test split		Challenge split		
	Tight (1–5 s)	Loose (5–60 s)	Tight (1–5 s)	Shown	Unshown
RMS-Net [57]	28.83	63.49	27.69	-	-
NetVLAD++ [22]	-	-	43.99	-	-
Zhou et al. [71] (2021 challenge; 1st)	47.05	73.77	49.56	54.42	45.42
‡Soares et al. [51] (2022 challenge; 1st)	-	-	‡ 67.81	‡72.84	‡ 60.17
E2E-Spot 200MF	61.19	73.25	63.28	70.41	45.98
E2E-Spot 800MF	61.82	74.05	66.01	72.76	51.65
‡E2E-Spot 800MF (2022 challenge; 2nd)	-	-	‡66.73	‡ 74.84	‡53.21

5.3 Additional Variations of E2E-Spot

More Complex Architectures, G . Prior TAD and TAS works catalog a rich history of head architectures (see related; § 2) operating on pre-extracted features. We examine whether these architectures can directly benefit from end-to-end learning with E2E-Spot by replacing the 1-layer GRU. Table 3d shows that improvement is not guaranteed; MS-TCN, ASFormer, and deeper GRUs neither consistently nor significantly outperform a single layer GRU. This suggests that *end-to-end learned spatial-temporal features can already capture much of the logic previously handled by the downstream architecture.*

Enhancements to Feature Extractor, F . We explore two basic enhancements to F that do not require new assumptions or domain knowledge: a larger CNN backbone (such as RegNet-Y 800MF) and optical flow [55] input. Table 3e shows that these enhancements can yield modest improvements (up to 4.4 mAP on FineGym). Flow, by itself, is worse than RGB but can improve results when ensembled with RGB. Larger models show promise on some datasets, but the improvements are not as significant as the lift from end-to-end learning.

5.4 Results on the SoccerNet Action Spotting Challenge

E2E-Spot also generalizes to temporally coarse spotting tasks, such as SoccerNet-v2 [13], which studies 17 action classes in 550 matches — split across train / val / test / challenge sets. As in prior work [9, 22, 57], we extract frames at 2 FPS and evaluate using average-mAP across tolerances, defined as $\pm\delta/2$ second ranges around events. In Table 4, we compare E2E-Spot to the best results from the CVPR 2021 (lenient tolerances of 5–60 sec) and CVPR 2022 (less coarse, 1–5 sec tolerances) SoccerNet Action Spotting challenges [14].

E2E-Spot, with the 200MF CNN, matches the top prior method from the 2021 competition [71] in the 5–60 sec setting while outperforming it by 13.7–14.1

avg-mAP points in the less coarse, 1–5 sec setting. Increasing the CNN to 800MF improves avg-mAP slightly (by 0.4–2.7 avg-mAP). E2E-Spot places second in the (concurrent) 2022 competition (within 1.1 avg-mAP), after Soares et al. [51], due to the latter’s strong performance on unshown actions (not visible in the frame). Soares et al. [51, 52] and Zhou et al. [71] are two-phase approaches, combining pre-extracted features from multiple (5 to 6) heterogeneous, fine-tuned feature extractors and proposing downstream architectures and losses on those features. In contrast, E2E-Spot shows that direct, end-to-end training of a simple and compact model can be a surprisingly strong baseline.

6 Discussion and Future Work

In this paper, we have presented a from-the-ground-up study of end-to-end feature learning for spotting in the temporally stringent setting.

E2E-Spot is a simple baseline that obtains competitive or state-of-the-art performance on temporally precise (and coarser) spotting tasks, outperforming conventional approaches derived from related work on TAD and TAS (§ 2). The secondary benefits we obtain from end-to-end learning are a simplified analysis pipeline, trained in a single phase under direct supervision, and the ability to use smaller, simpler models, without sacrificing accuracy on the frame-accurate task. Methodological enhancements such as improved architectures (e.g., based on ViT [17]) for feature extraction, training methodologies, head architectures, and losses that benefit from end-to-end learning are interesting research directions. We hope that E2E-Spot serves as a principled baseline for this future work.

Video understanding encapsulates a broad body of tasks, of which spotting frame-accurate events is a single example. We consider it future work to analyze other tasks and their datasets, and we anticipate situations where end-to-end learning alone may be insufficient: e.g., when reliable priors such as pose are readily available, or when training data is limited or exhibits domain-shift in the pixel domain. Learning to spot accurately with few or weak labels will accelerate the curation new datasets for more advanced, downstream video analysis tasks.

7 Conclusion

We have introduced temporally precise spotting in video, supported by four fine-grained sports datasets. Many recent advances in TAD, TAS, and spotting trend towards increasingly complex models and processing pipelines, which generalize poorly for this strict, but practical setting. E2E-Spot shows that a few key design principles — task-specialized spatial-temporal features, reasoning over sufficient temporal context, and efficient end-to-end learning — can go a long way for improving accuracy and simplifying solutions.

Acknowledgements. This work is supported by the National Science Foundation (NSF) under III-1908727, Intel Corporation, and Adobe Research. We also thank the anonymous reviewers for their comments and feedback.

References

1. Ahn, H., Lee, D.: Refining action segmentation with hierarchical video representations. In: Proceedings of the IEEE/CVF International Conference on Computer Vision (ICCV). pp. 16302–16310 (October 2021)
2. Alwassel, H., Giancola, S., Ghanem, B.: TSP: Temporally-sensitive pretraining of video encoders for localization tasks. In: Proceedings of the IEEE/CVF International Conference on Computer Vision (ICCV) Workshops. pp. 3173–3183 (October 2021)
3. Buch, S., Escorcia, V., Ghanem, B., Niebles, J.C.: End-to-end, single-stream temporal action detection in untrimmed videos. In: Proceedings of the British Machine Vision Conference (BMVC) (September 2017)
4. Buch, S., Escorcia, V., Shen, C., Ghanem, B., Carlos Niebles, J.: SST: Single-stream temporal action proposals. In: Proceedings of the IEEE Conference on Computer Vision and Pattern Recognition (CVPR) (July 2017)
5. Caba Heilbron, F., Escorcia, V., Ghanem, B., Carlos Niebles, J.: ActivityNet: A large-scale video benchmark for human activity understanding. In: Proceedings of the IEEE Conference on Computer Vision and Pattern Recognition (CVPR) (June 2015)
6. Carreira, J., Zisserman, A.: Quo vadis, action recognition? A new model and the Kinetics dataset. In: Proceedings of the IEEE Conference on Computer Vision and Pattern Recognition (CVPR) (July 2017)
7. Chen, M.H., Li, B., Bao, Y., AlRegib, G.: Action segmentation with mixed temporal domain adaptation. In: Proceedings of the IEEE/CVF Winter Conference on Applications of Computer Vision (WACV) (March 2020)
8. Chung, J., Gulcehre, C., Cho, K., Bengio, Y.: Empirical evaluation of gated recurrent neural networks on sequence modeling. In: Proceedings of NIPS Deep Learning and Representation Learning Workshop (2014)
9. Cioppa, A., Deliege, A., Giancola, S., Ghanem, B., Van Droogenbroeck, M., Gade, R., Moeslund, T.B.: A context-aware loss function for action spotting in soccer videos. In: IEEE/CVF Conference on Computer Vision and Pattern Recognition (CVPR) (June 2020)
10. Dai, R., Das, S., Minciullo, L., Garattoni, L., Francesca, G., Bremond, F.: PDAN: Pyramid dilated attention network for action detection. In: Proceedings of the IEEE/CVF Winter Conference on Applications of Computer Vision (WACV). pp. 2970–2979 (January 2021)
11. Dai, R., Das, S., Sharma, S., Minciullo, L., Garattoni, L., Bremond, F., Francesca, G.: Toyota Smarthome Untrimmed: Real-world untrimmed videos for activity detection (2020), arXiv:2010.14982
12. Damen, D., Doughty, H., Farinella, G.M., Fidler, S., Furnari, A., Kazakos, E., Moltisanti, D., Munro, J., Perrett, T., Price, W., Wray, M.: Scaling egocentric vision: The EPIC-KITCHENS dataset. In: Proceedings of the European Conference on Computer Vision (ECCV) (September 2018)
13. Deliege, A., Cioppa, A., Giancola, S., Seikavandi, M.J., Dueholm, J.V., Nasrollahi, K., Ghanem, B., Moeslund, T.B., Van Droogenbroeck, M.: SoccerNet-v2: A dataset and benchmarks for holistic understanding of broadcast soccer videos. In: Proceedings of the IEEE/CVF Conference on Computer Vision and Pattern Recognition (CVPR) Workshops. pp. 4508–4519 (June 2021)
14. Deliege, A., Cioppa, A., Giancola, S., Seikavandi, M.J., Dueholm, J.V., Nasrollahi, K., Ghanem, B., Moeslund, T.B., Droogenbroeck, M.V.: SoccerNet - action spotting. <https://github.com/SoccerNet/sn-spotting> (2022)

15. Deng, J., Dong, W., Socher, R., Li, L.J., Li, K., Fei-Fei, L.: ImageNet: A large-scale hierarchical image database. In: Proceedings of the IEEE/CVF Conference on Computer Vision and Pattern Recognition (CVPR) (June 2009)
16. Ding, L., Xu, C.: TricorNet: A hybrid temporal convolutional and recurrent network for video action segmentation (2017), arXiv:1705.07818
17. Dosovitskiy, A., Beyer, L., Kolesnikov, A., Weissenborn, D., Zhai, X., Unterthiner, T., Dehghani, M., Minderer, M., Heigold, G., Gelly, S., Uszkoreit, J., Houlsby, N.: An image is worth 16x16 words: Transformers for image recognition at scale. In: International Conference on Learning Representations (ICLR) (2021)
18. Fan, H., Xiong, B., Mangalam, K., Li, Y., Yan, Z., Malik, J., Feichtenhofer, C.: Multiscale vision transformers. In: Proceedings of the IEEE/CVF International Conference on Computer Vision (ICCV). pp. 6824–6835 (October 2021)
19. Farha, Y.A., Gall, J.: MS-TCN: Multi-stage temporal convolutional network for action segmentation. In: Proceedings of the IEEE/CVF Conference on Computer Vision and Pattern Recognition (CVPR) (June 2019)
20. Fathi, A., Ren, X., Rehg, J.M.: Learning to recognize objects in egocentric activities. In: Proceedings of the IEEE/CVF Conference on Computer Vision and Pattern Recognition (CVPR) (June 2011)
21. Feichtenhofer, C., Fan, H., Malik, J., He, K.: SlowFast networks for video recognition. In: Proceedings of the IEEE/CVF International Conference on Computer Vision (ICCV) (October 2019)
22. Giancola, S., Ghanem, B.: Temporally-aware feature pooling for action spotting in soccer broadcasts. In: Proceedings of the IEEE/CVF Conference on Computer Vision and Pattern Recognition (CVPR) Workshops. pp. 4490–4499 (June 2021)
23. Girshick, R., Donahue, J., Darrell, T., Malik, J.: Rich feature hierarchies for accurate object detection and semantic segmentation. In: Proceedings of the IEEE Conference on Computer Vision and Pattern Recognition (CVPR) (June 2014)
24. Hao, Y., Zhang, H., Ngo, C.W., Liu, Q., Hu, X.: Compact bilinear augmented query structured attention for sport highlights classification. In: Proceedings of the 28th ACM International Conference on Multimedia. pp. 628–636. Association for Computing Machinery, New York, NY, USA (2020)
25. Hong, J., Fisher, M., Gharbi, M., Fatahalian, K.: Video pose distillation for few-shot, fine-grained sports action recognition. In: Proceedings of the IEEE/CVF International Conference on Computer Vision (ICCV). pp. 9254–9263 (October 2021)
26. Ibrahim, M.S., Muralidharan, S., Deng, Z., Vahdat, A., Mori, G.: A hierarchical deep temporal model for group activity recognition. In: Proceedings of the IEEE Conference on Computer Vision and Pattern Recognition (CVPR) (June 2016)
27. Ishikawa, Y., Kasai, S., Aoki, Y., Kataoka, H.: Alleviating over-segmentation errors by detecting action boundaries. In: Proceedings of the IEEE/CVF Winter Conference on Applications of Computer Vision (WACV). pp. 2322–2331 (January 2021)
28. Jiang, Y.G., Liu, J., Roshan Zamir, A., Toderici, G., Laptev, I., Shah, M., Suthankar, R.: THUMOS Challenge: Action recognition with a large number of classes (2014)
29. Kay, W., Carreira, J., Simonyan, K., Zhang, B., Hillier, C., Vijayanarasimhan, S., Viola, F., Green, T., Back, T., Natsev, P., Suleyman, M., Zisserman, A.: The Kinetics human action video dataset (2017), arXiv:1705.06950
30. Kuehne, H., Arslan, A., Serre, T.: The language of actions: Recovering the syntax and semantics of goal-directed human activities. In: Proceedings of the IEEE Conference on Computer Vision and Pattern Recognition (CVPR) (June 2014)

31. Li, A., Thotakuri, M., Ross, D.A., Carreira, J., Vostrikov, A., Zisserman, A.: The AVA-Kinetics localized human actions video dataset (2020), arXiv:2005.00214
32. Li, Y., Li, Y., Vasconcelos, N.: RESOUND: Towards action recognition without representation bias. In: Proceedings of the European Conference on Computer Vision (ECCV) (September 2018)
33. Li, Y., Chen, L., He, R., Wang, Z., Wu, G., Wang, L.: MultiSports: A multi-person video dataset of spatio-temporally localized sports actions. In: Proceedings of the IEEE/CVF International Conference on Computer Vision (ICCV). pp. 13536–13545 (October 2021)
34. Lin, C., Xu, C., Luo, D., Wang, Y., Tai, Y., Wang, C., Li, J., Huang, F., Fu, Y.: Learning salient boundary feature for anchor-free temporal action localization. In: Proceedings of the IEEE/CVF Conference on Computer Vision and Pattern Recognition (CVPR). pp. 3320–3329 (June 2021)
35. Lin, J., Gan, C., Han, S.: TSM: Temporal shift module for efficient video understanding. In: Proceedings of the IEEE/CVF International Conference on Computer Vision (ICCV) (October 2019)
36. Lin, T., Liu, X., Li, X., Ding, E., Wen, S.: BMN: Boundary-matching network for temporal action proposal generation. In: Proceedings of the IEEE/CVF International Conference on Computer Vision (ICCV) (October 2019)
37. Lin, T., Zhao, X., Su, H., Wang, C., Yang, M.: BSN: Boundary sensitive network for temporal action proposal generation. In: Proceedings of the European Conference on Computer Vision (ECCV) (September 2018)
38. Liu, X., Bai, S., Bai, X.: An empirical study of end-to-end temporal action detection. In: Proceedings of the IEEE/CVF Conference on Computer Vision and Pattern Recognition (CVPR). pp. 20010–20019 (June 2022)
39. Liu, X., Hu, Y., Bai, S., Ding, F., Bai, X., Torr, P.H.S.: Multi-shot temporal event localization: A benchmark. In: Proceedings of the IEEE/CVF Conference on Computer Vision and Pattern Recognition (CVPR). pp. 12596–12606 (June 2021)
40. Loshchilov, I., Hutter, F.: SGDR: Stochastic gradient descent with warm restarts. In: Proceedings of the International Conference on Learning Representations (ICLR) (2017)
41. Loshchilov, I., Hutter, F.: Decoupled weight decay regularization. In: Proceedings of the International Conference on Learning Representations (ICLR) (2019)
42. Nvidia: Nvidia RTX A5000 data sheet (2021)
43. Radosavovic, I., Kosaraju, R.P., Girshick, R., He, K., Dollar, P.: Designing network design spaces. In: Proceedings of the IEEE/CVF Conference on Computer Vision and Pattern Recognition (CVPR) (June 2020)
44. Shao, D., Zhao, Y., Dai, B., Lin, D.: FineGym: A hierarchical video dataset for fine-grained action understanding. In: Proceedings of the IEEE/CVF Conference on Computer Vision and Pattern Recognition (CVPR) (June 2020)
45. Sigurdsson, G., Choi, J.: Charades Challenge (2017)
46. Sigurdsson, G.A., Divvala, S., Farhadi, A., Gupta, A.: Asynchronous temporal fields for action recognition. In: Proceedings of the IEEE Conference on Computer Vision and Pattern Recognition (CVPR) (July 2017)
47. Sigurdsson, G.A., Varol, G., Wang, X., Farhadi, A., Laptev, I., Gupta, A.: Hollywood in homes: Crowdsourcing data collection for activity understanding. In: Proceedings of the European Conference on Computer Vision (ECCV) (September 2016)
48. Singh, B., Marks, T.K., Jones, M., Tuzel, O., Shao, M.: A multi-stream bi-directional recurrent neural network for fine-grained action detection. In: Pro-

- ceedings of the IEEE Conference on Computer Vision and Pattern Recognition (CVPR) (June 2016)
49. Singh, B., Marks, T.K., Jones, M., Tuzel, O., Shao, M.: A multi-stream bi-directional recurrent neural network for fine-grained action detection. In: Proceedings of the IEEE Conference on Computer Vision and Pattern Recognition (CVPR) (June 2016)
 50. Singhanian, D., Rahaman, R., Yao, A.: Coarse to fine multi-resolution temporal convolutional network (2021), arXiv:2105.10859
 51. Soares, J.V.B., Shah, A.: Action spotting using dense detection anchors revisited: Submission to the SoccerNet Challenge 2022 (2022), arXiv:2206.07846
 52. Soares, J.V.B., Shah, A., Biswas, T.: Temporally precise action spotting in soccer videos using dense detection anchors (2022), arXiv:2205.10450
 53. Stein, S., McKenna, S.J.: Combining embedded accelerometers with computer vision for recognizing food preparation activities. In: Proceedings of ACM International Joint Conference on Pervasive and Ubiquitous Computing (UbiComp). pp. 729–738. Association for Computing Machinery, New York, NY, USA (2013)
 54. Sudhakaran, S., Escalera, S., Lanz, O.: Gate-shift networks for video action recognition. In: Proceedings of the IEEE/CVF Conference on Computer Vision and Pattern Recognition (CVPR) (June 2020)
 55. Teed, Z., Deng, J.: RAFT: Recurrent all-pairs field transforms for optical flow. In: Proceedings of the European Conference on Computer Vision (ECCV) (August 2020)
 56. Tirupattur, P., Duarte, K., Rawat, Y.S., Shah, M.: Modeling multi-label action dependencies for temporal action localization. In: Proceedings of the IEEE/CVF Conference on Computer Vision and Pattern Recognition (CVPR). pp. 1460–1470 (June 2021)
 57. Tomei, M., Baraldi, L., Calderara, S., Bronzin, S., Cucchiara, R.: RMS-Net: Regression and masking for soccer event spotting. In: 2020 25th International Conference on Pattern Recognition (ICPR). pp. 7699–7706. IEEE Computer Society, Los Alamitos, CA, USA (Jan 2021)
 58. Tran, D., Wang, H., Torresani, L., Ray, J., LeCun, Y., Paluri, M.: A closer look at spatiotemporal convolutions for action recognition. In: Proceedings of the IEEE Conference on Computer Vision and Pattern Recognition (CVPR) (June 2018)
 59. TwentyBN: The 20BN-something-something dataset v2
 60. Wang, L., Xiong, Y., Wang, Z., Qiao, Y., Lin, D., Tang, X., Val Gool, L.: Temporal segment networks: Towards good practices for deep action recognition. In: Proceedings of the European Conference on Computer Vision (ECCV) (September 2016)
 61. Xu, J., Rao, Y., Yu, X., Chen, G., Zhou, J., Lu, J.: FineDiving: A fine-grained dataset for procedure-aware action quality assessment. In: Proceedings of the IEEE/CVF Conference on Computer Vision and Pattern Recognition (CVPR). pp. 2949–2958 (June 2022)
 62. Xu, M., Zhao, C., Rojas, D.S., Thabet, A., Ghanem, B.: G-TAD: Sub-graph localization for temporal action detection. In: Proceedings of the IEEE/CVF Conference on Computer Vision and Pattern Recognition (CVPR) (June 2020)
 63. Yeung, S., Russakovsky, O., Jin, N., Andriluka, M., Mori, G., Fei-Fei, L.: Every moment counts: Dense detailed labeling of actions in complex videos. *International Journal of Computer Vision* **126**(2-4), 375–389 (2018)
 64. Yi, F., Wen, H., Jiang, T.: ASFormer: Transformer for action segmentation. In: Proceedings of the British Machine Vision Conference (BMVC) (November 2021)

65. Zeng, R., Huang, W., Tan, M., Rong, Y., Zhao, P., Huang, J., Gan, C.: Graph convolutional networks for temporal action localization. In: Proceedings of the IEEE/CVF International Conference on Computer Vision (ICCV) (October 2019)
66. Zhang, C., Wu, J., Li, Y.: ActionFormer: Localizing moments of actions with transformers (2022), arXiv:2202.07925
67. Zhang, H., Scutto, C., Agrawala, M., Fatahalian, K.: Vid2Player: Controllable video sprites that behave and appear like professional tennis players. *ACM Transactions on Graphics* **40**(3) (2021)
68. Zhang, H., Cisse, M., Dauphin, Y.N., Lopez-Paz, D.: mixup: Beyond empirical risk minimization. In: Proceedings of the International Conference on Learning Representations (ICLR) (2018)
69. Zhao, C., Thabet, A.K., Ghanem, B.: Video self-stitching graph network for temporal action localization. In: Proceedings of the IEEE/CVF International Conference on Computer Vision (ICCV). pp. 13658–13667 (October 2021)
70. Zhou, B., Andonian, A., Oliva, A., Torralba, A.: Temporal relational reasoning in videos. In: Proceedings of the European Conference on Computer Vision (ECCV) (September 2018)
71. Zhou, X., Kang, L., Cheng, Z., He, B., Xin, J.: Feature combination meets attention: Baidu soccer embeddings and transformer based temporal detection (2021), arXiv:2106.14447